

# Integration of [U-<sup>13</sup>C]glucose and <sup>2</sup>H<sub>2</sub>O for quantification of hepatic glucose production and gluconeogenesis

Rui Perdigoto,<sup>1</sup> Tiago B. Rodrigues,<sup>2</sup> Alexandre L. Furtado,<sup>1</sup> Armando Porto,<sup>1</sup> Carlos F. G. C. Geraldês<sup>2</sup> and John G. Jones<sup>2\*</sup>

<sup>1</sup>Medicine III, Transplantation Unit, University Hospital of Coimbra, 3049, Coimbra, Portugal

<sup>2</sup>Department of Biochemistry and Center for Neuroscience and Cell Biology, Faculty of Sciences and Technology, Box 3126, University of Coimbra, 3001-401, Coimbra, Portugal

Received 19 November 2002; Revised 8 May 2003; Accepted 13 May 2003

**ABSTRACT:** Glucose metabolism in five healthy subjects fasted for 16 h was measured with a combination of [U-<sup>13</sup>C]glucose and <sup>2</sup>H<sub>2</sub>O tracers. Phenylbutyric acid was also provided to sample hepatic glutamine for the presence of <sup>13</sup>C-isotopomers derived from the incorporation of [U-<sup>13</sup>C]glucose products into the hepatic Krebs cycle. Glucose production (GP) was quantified by <sup>13</sup>C NMR analysis of the monoacetone derivative of plasma glucose following a primed infusion of [U-<sup>13</sup>C]glucose and provided reasonable estimates (1.90 ± 0.19 mg/kg/min with a range of 1.60–2.15 mg/kg/min). The same derivative yielded measurements of plasma glucose <sup>2</sup>H-enrichment from <sup>2</sup>H<sub>2</sub>O by <sup>2</sup>H NMR from which the contribution of glycogenolytic and gluconeogenic fluxes to GP was obtained (0.87 ± 0.14 and 1.03 ± 0.10 mg/kg/min, respectively). Hepatic glutamine <sup>13</sup>C-isotopomers representing multiply-enriched oxaloacetate and [U-<sup>13</sup>C]acetyl-CoA were identified as multiplets in the <sup>13</sup>C NMR signals of the glutamine moiety of urinary phenylacetylglutamine, demonstrating entry of the [U-<sup>13</sup>C]glucose tracer into both oxidative and anaplerotic pathways of the hepatic Krebs cycle. These isotopomers contributed 0.1–0.2% excess enrichment to carbons 2 and 3 and ~0.05% to carbon 4 of glutamine. Copyright © 2003 John Wiley & Sons, Ltd.

**KEYWORDS:** phenylacetylglutamine; <sup>2</sup>H NMR; <sup>13</sup>C NMR; isotopomers; gluconeogenesis; Krebs cycle

## INTRODUCTION

In the postabsorptive state, endogenous glucose production (GP) is sustained by a combination of glycogenolysis and gluconeogenesis. These fluxes can now be measured in a standard clinical setting by ingestion of <sup>2</sup>H<sub>2</sub>O<sup>1–4</sup> followed by an isotope dilution measurement of glucose turnover once plasma glucose <sup>2</sup>H-enrichment from <sup>2</sup>H<sub>2</sub>O has reached steady state.<sup>1,2,4</sup> Glucose turnover is obtained by a primed infusion of a non-recyclable glucose tracer such as [1,6-<sup>13</sup>C<sub>2</sub>]glucose,<sup>2</sup> or [6,6-<sup>2</sup>H<sub>2</sub>]glucose.<sup>1,4</sup> Enrichment of plasma glucose from both tracers is then resolved and quantified from a single set of blood

samples obtained at the end of the glucose turnover measurement. The ratio of <sup>2</sup>H-enrichment in positions 5 and 2 of plasma glucose from ingested <sup>2</sup>H<sub>2</sub>O provides a measure of the fraction of GP derived from gluconeogenesis and glycogenolysis.<sup>1–4</sup> Meanwhile, the enrichment level of the infused glucose tracer allows glucose turnover and the absolute rate of GP to be estimated.<sup>1–4</sup> Absolute gluconeogenic flux is thus estimated as the product of absolute GP and the fraction of GP derived from gluconeogenesis, while absolute glycogenolytic flux is the difference between the absolute rates of GP and gluconeogenesis.<sup>1,2,4</sup> Mass spectrometry (MS) procedures have been developed for quantifying and resolving plasma glucose enrichment from a mixture of <sup>2</sup>H<sub>2</sub>O and [6,6-<sup>2</sup>H<sub>2</sub>]glucose.<sup>1,4</sup> While this approach is highly sensitive and utilizes a relatively inexpensive tracer of glucose turnover, the derivatization procedure is laborious and difficult to routinely implement in a clinical laboratory setting.<sup>1,3–5</sup> Alternatively, <sup>2</sup>H NMR analysis of a monoacetone glucose derivative (MAG) of plasma glucose<sup>6,7</sup> is less sensitive but much simpler to perform and provides <sup>2</sup>H enrichment information for all positions of glucose. Note that <sup>2</sup>H NMR cannot resolve deuterium isotopomers of glucose, thereby precluding measurement of GP with [6,6-<sup>2</sup>H<sub>2</sub>]glucose in the presence of glucose

\*Correspondence to: J. G. Jones, Center for Neurosciences and Cell Biology, NMR Center, Department of Biochemistry, Faculty of Sciences and Technology, University of Coimbra, 3001-401 Coimbra, Portugal. E-mail: jones@cnc.cj.uc.pt

Contract/grant sponsor: European Community Marie Curie Experienced Researcher Fellowship; contract/grant number: MCF-2000-00148.

Contract/grant sponsor: Portuguese Foundation of Science and Technology.

**Abbreviations used:** GP, glucose production; HSQC, heteronuclear single quantum coherence; MAG, monoacetone glucose; MS, mass spectrometry; OAA, oxaloacetate; PAGN, phenylacetylglutamine; PEP, phosphoenolpyruvate.

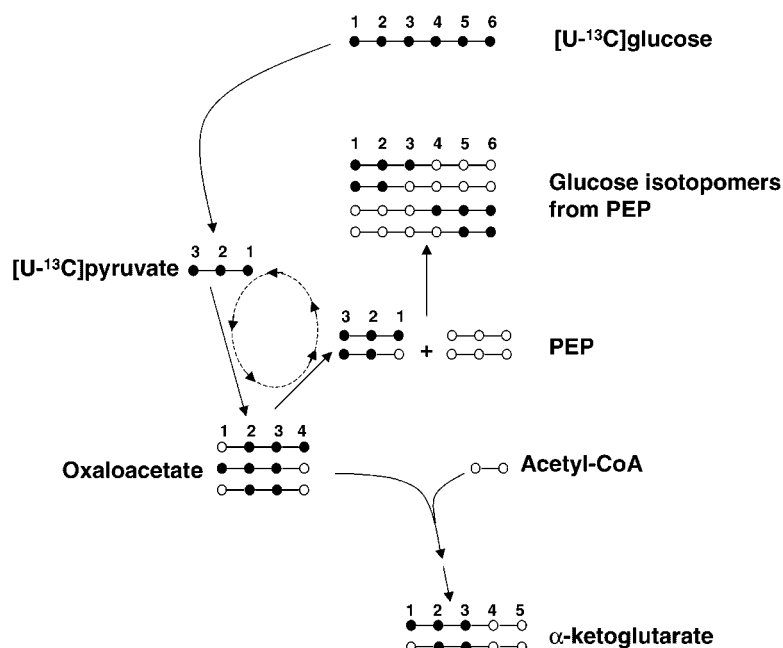


**Figure 1.** Fate of the  $^{13}C$  of infused  $[U-^{13}C]$ glucose. Glycolysis in peripheral tissues generates  $[U-^{13}C]$ pyruvate and its equivalents. These are transported to liver and enter the hepatic Krebs cycle, principally as anaplerotic carbons via pyruvate carboxylase. Following carboxylation of  $[U-^{13}C]$ pyruvate, the initial  $[2,3,4-^{13}C_3]$ OAA product undergoes rapid exchange with malate and fumarate, resulting in  $\sim 50\%$  conversion to  $[1,2,3-^{13}C_3]$ OAA. Both isotopomers can be converted to  $[2,3-^{13}C_2]$ OAA as a result of the de-carboxylation and re-carboxylation reactions of pyruvate recycling (dotted arrows) coupled with  $OAA \leftrightarrow MAL \leftrightarrow FUM$  exchange.<sup>19</sup> Gluconeogenic outflow generates  $[U-^{13}C]$  and  $[2,3-^{13}C_2]$ PEP and the corresponding  $[1,2,3-^{13}C_3]$ - and  $[1,2-^{13}C_2]$ glucose isotopomers. These account for the majority ( $\sim 85\%$ ) of glucose  $^{13}C$ -enrichment derived from gluconeogenesis of  $[U-^{13}C]$ pyruvate.<sup>29,30</sup> The corresponding  $\alpha$ -ketoglutarate isotopomers generated from condensation of the OAA isotopomers with unlabeled acetyl-CoA are also shown

enrichment from  $^2H_2O$ .<sup>\*</sup> However,  $^2H$  enrichment and  $^{13}C$  isotopomers can be resolved by NMR, allowing GP to be quantified with an alternative  $^{13}C$ -tracer such as  $[1,6-^{13}C_2]$ glucose.<sup>2</sup> This approach would be considerably simplified if all  $^2H$  enrichment and  $^{13}C$  isotopomer information could be obtained from a single MAG derivative. This cannot be accomplished with  $[1,6-^{13}C_2]$ glucose because spin-spin coupling between carbons 1 and 6 of glucose is abolished following its conversion to MAG. However, MAG features  $^{13}C$ - $^{13}C$  couplings that are favorable for resolving and quantifying a number of other glucose  $^{13}C$ -isotopomers including  $[U-^{13}C]$ glucose, a widely used  $^{13}C$  tracer of GP. Therefore, a principal goal of this study was to administer a combination of  $^2H_2O$  and  $[U-^{13}C]$ glucose and quantify  $^2H$ -enrichment levels and glucose  $^{13}C$ -isotopomer distributions by sequential  $^2H$  and  $^{13}C$  NMR analysis of MAG.

<sup>\*</sup>There is no significant spin-spin coupling between adjacent deuterium nuclei in either the glucose or monoacetone glucose molecule hence  $[6,6-^2H_2]$ glucose cannot be resolved from a mixture of  $[6R-^2H]$  and  $[6S-^2H]$ glucose by  $^2H$  NMR.

This provides estimates of GP and its component fluxes from glycogen and gluconeogenesis from a single NMR sample.

In addition to providing estimates of GP in humans,  $[U-^{13}C]$ glucose is also a potential hepatic Krebs cycle tracer as a consequence of carbon recycling (glucose  $\rightarrow$  pyruvate  $\rightarrow$  glucose) via the Cori and glucose-alanine cycles. Resolution and quantification of glucose triose  $^{13}C$ -isotopomers formed by recycling has been used to estimate the fractional contribution of gluconeogenesis to GP.<sup>8</sup> However, this measurement is fraught with both physiological and methodological uncertainties<sup>9-13</sup> and in any event is made redundant by the metabolic information derived from  $^2H_2O$ . Nevertheless, the presence of glucose triose isotopomers is proof that the  $^{13}C$  label must have entered the hepatic Krebs cycle. This is because  $[U-^{13}C]$ glucose is converted to  $[U-^{13}C]$ pyruvate by glycolysis in peripheral tissues and the  $[U-^{13}C]$ pyruvate moiety is then exported to the liver as lactate or alanine. Here, its principal fate is conversion to oxaloacetate (OAA) via pyruvate carboxylase. This results in the passage of uniformly labeled pyruvate moieties

through the hepatic Krebs cycle and gluconeogenic pathways, giving rise to a mixture of phosphoenolpyruvate (PEP) isotopomers which propagate into both triose moieties of plasma glucose (see Fig. 1). The  $^{13}\text{C}$ -isotopomer distributions of OAA and other Krebs cycle intermediates are also preserved in the carbon skeletons of aspartate, glutamate and glutamine. This was demonstrated in pigs infused with  $[\text{U-}^{13}\text{C}]\text{glucose}$ ,<sup>14</sup> but to our knowledge it has not been established in humans. Human hepatic glutamine can be safely assayed by ingestion of phenylacetic or phenylbutyric acid, and the  $^{13}\text{C}$  isotopomer distribution of the glutamine moiety characterized by  $^{13}\text{C}$  NMR of urinary phenylacetylglutamine (PAGN).<sup>2,15</sup> Hepatic glutamine  $^{13}\text{C}$  isotopomer analysis provides a comprehensive assessment of Krebs cycle fluxes that can be integrated with measurements of GP and gluconeogenesis.<sup>2</sup> To determine if hepatic glutamine  $^{13}\text{C}$ -isotopomer information could be obtained in this manner from  $[\text{U-}^{13}\text{C}]\text{glucose}$ , we supplemented the tracers with oral phenylbutyrate and analyzed urinary PAGN by  $^{13}\text{C}$  NMR.

## MATERIALS AND METHODS

### Human studies

All subjects were studied with a protocol approved by the University of Coimbra Hospital Ethics Committee and all gave informed consent prior to admission into the study. The group consisted of five healthy subjects, three males and two females with a mean age of  $25 \pm 7$  years (range 19–39 years) and mean weight of  $68 \pm 10$  kg (range 54–78 kg).

Subjects began fasting at 20:00. During the fast, they ingested a quantity of sterile and pyrogen-free 70%  $^2\text{H}_2\text{O}$  to attain body water enrichment of  $\sim 0.5\%$ . For each subject, the amount of 70%-enriched  $^2\text{H}_2\text{O}$  required to achieve 0.5% body water enrichment was  $\sim 260$  ml. To reduce the possibility of vertigo, this was divided into two portions of  $\sim 130$  ml, each taken at 01:00 and 06:00 (5 and 10 h into the fast). For the remainder of the study, all subjects ingested 0.5%  $^2\text{H}_2\text{O}$  *ad libitum*. At 08:00 the next day, a 4 h primed infusion of sterile and pyrogenfree  $[\text{U-}^{13}\text{C}]\text{glucose}$  (4.7 mg/kg prime,  $\sim 0.060$  mg/kg/min) into a peripheral forearm vein was initiated. Subjects ingested 250–500 mg phenylbutyric acid packaged in gelatin capsules at 09:40, 10:00 and 10:20, for a total of 0.75–1.5 g. At 11:00, 11:20, 11:40 and 12:00, 20 ml of blood were drawn from a contralateral vein. Urine was collected from 10:30 to 12:00 after which the study was concluded.

### Sampling processing

Blood was stored at  $4^\circ\text{C}$  and centrifuged within 2 h of being drawn. For some samples, the plasma supernatant

protein was precipitated by centrifugation following addition of one-tenth the plasma volume of 70% perchloric acid. The supernatant was neutralized with KOH and lyophilized following centrifugation of precipitated  $\text{KClO}_4$ . For the remaining samples, plasma protein was precipitated by the addition of 4 vols methanol per volume of plasma and the supernatant was recovered by filtration via a Buchner funnel. The methanol was removed by rotary evaporation at  $40^\circ\text{C}$  after which the remaining aqueous fraction was removed by lyophilization. For conversion of plasma glucose to the monoacetone derivative, the lyophilized extracts were treated with 3–20 ml anhydrous acetone enriched to 0.15% with acetone- $d_6$  to which concentrated sulfuric acid (4% v/v) was added. The solution was quickly cooled to room temperature, and MAG was prepared for NMR analysis as described.<sup>16</sup>

Urine samples were adjusted to pH 7.0 and incubated overnight with 10000 U of urease per sample. A trace of sodium azide was also added to inhibit possible infection from airborne microorganisms. The samples were then depleted of protein by addition of perchloric acid, followed by neutralization, centrifugation and lyophilization. Upon reconstitution in 2–3 ml water, the pH was adjusted to 8.0, the sample loaded on to a 5 ml Dowex-1  $\times$  8-acetate column and washed with 25 ml of water. PAGN was eluted with 15 ml of 10 M acetic acid. This fraction was evaporated and re-suspended in 0.5–1.0 ml water. The pH was adjusted to 7.0 with NaOH, and the samples were centrifuged in Eppendorf tubes. A 0.5 ml aliquot of the supernatant was introduced into a 5 mm NMR tube and 100  $\mu\text{l}$  of  $\text{CD}_3\text{CN}$  were added to provide a deuterium signal for lock and shimming.

### NMR spectroscopy

$^2\text{H}$  NMR spectra of urine water and MAG were acquired at 11.75 T with a Varian Unity 500 system equipped with a 5 mm broadband 'switchable' probe with z-gradient (Varian, Palo Alto, CA, USA) as described.<sup>17</sup> Absolute enrichment of glucose hydrogen 2 in selected MAG samples was obtained by addition of a  $^2\text{H}$ -formate standard of known enrichment to the NMR sample.<sup>16</sup>  $^{13}\text{C}$  NMR spectra of MAG were obtained following addition of 100  $\mu\text{l}$   $\text{CD}_3\text{CN}$  to provide a lock signal.  $^{13}\text{C}$  NMR spectra of PAGN were obtained following addition of 100  $\mu\text{l}$   $\text{CD}_3\text{CN}$  to a neutral, aqueous solution of PAGN in  $\sim 1.0$  ml distilled water and incorporation of 0.6 ml of this mixture into a 5 mm NMR tube. In all cases, partially saturated  $^{13}\text{C}$  NMR spectra were obtained with an acquisition time of 2 s and a pulse delay of 1 s. The number of acquisitions ranged from 5000 to 25000. For some samples, and for MAG prepared from  $[\text{U-}^{13}\text{C}]\text{glucose}$  of the infusion solution, quantification of carbon 1 enrichment was performed by  $^1\text{H}$  NMR. This was achieved by pre-saturation of the acetonitrile signal and

applying selective  $^{13}\text{C}$ -decoupling in the 65–85 ppm spectral window. The decoupling procedure improves the resolution of the  $^{13}\text{C}$ -satellite signals by removing long-range  $^{13}\text{C}$ – $^1\text{H}$  couplings between hydrogen 1 and carbons 2–6 while retaining the direct coupling between  $^{13}\text{C}$  and  $^1\text{H}$  in position 1.<sup>17</sup> For all plasma glucose samples, MAG carbon 1  $^{13}\text{C}$ -enrichment was quantified from its  $^{13}\text{C}$  NMR spectrum using the approach of Brainard *et al.*<sup>18</sup> Here, the intensity of the  $^{13}\text{C}$  singlet component of any given glucose resonance is assumed to represent the natural abundance  $^{13}\text{C}$ -enrichment of 1.11%. The intensity of a  $^{13}\text{C}$ – $^{13}\text{C}$  spin-coupled multiplet signal is expressed as fractional  $^{13}\text{C}$  enrichment by obtaining the ratio of the multiplet and singlet signal and multiplying by 1.11%. For example, if a glucose  $^{13}\text{C}$  resonance features a multiplet whose intensity is twice that of the singlet, then the percentage  $^{13}\text{C}$ -enrichment represented by the glucose  $^{13}\text{C}$ -isotopomers that contribute to that multiplet signal will be  $2 \times 1.11 = 2.22\%$ . Deuterium enrichment of body water was determined by  $^2\text{H}$  NMR analysis of plasma and urine  $^2\text{H}$  water enrichment as previously described.<sup>16</sup>

Sterile and pyrogen-free  $[\text{U-}^{13}\text{C}]\text{glucose}$  was obtained from Cambridge Isotopes (Cambridge, MA, USA). Sterile and pyrogen-free 70%  $^2\text{H}_2\text{O}$  was obtained from Cambridge Isotopes and Eurisotop, Gif-sur-Yvette, France. All NMR spectra were analyzed using the curve-fitting routine supplied with the NUTS PC-based NMR spectral analysis program (Acorn NMR Inc., Fremont, CA, USA).

## Calculations

Total  $^{13}\text{C}$ -enrichment of plasma glucose carbon 1 and enrichment of the  $[\text{U-}^{13}\text{C}]\text{glucose}$  isotopomer were determined from the carbon 1 multiplet of MAG. The singlet fraction ( $S$ ) is assumed to be derived from natural abundance  $^{13}\text{C}$  and is assigned an enrichment value of 1.11%.<sup>18</sup> The Q125 signal is assumed to reflect contribution from  $[\text{U-}^{13}\text{C}]\text{glucose}$ . Therefore, the enrichment of level of plasma  $[\text{U-}^{13}\text{C}]\text{glucose}$  ( $E_p$ ) is simply related to the ratio of the Q125 and  $S$  signals.

$$\text{Plasma glucose enrichment (\%)} = 1/S \times 1.11$$

$$\text{Plasma}[\text{U-}^{13}\text{C}]\text{glucose enrichment,}$$

$$E_p(\%) = Q125/S \times 1.11$$

GP was calculated as follows:

$$\text{GP} = [i \times (E_i/E_p)] - i$$

where  $i$  = infusion rate of  $[\text{U-}^{13}\text{C}]\text{glucose}$ , and  $E_i$  and  $E_p$  = percentage enrichment of infusate and plasma  $[\text{U-}^{13}\text{C}]\text{glucose}$ , respectively.

Relative rates of glycogenolysis and gluconeogenesis from glycerol and the Krebs cycle were estimated from

$^2\text{H}$ -enrichment of hydrogens 2, 5 and 6S of glucose ( $H2$ ,  $H5$  and  $H6S$ ) as determined by  $^2\text{H}$  NMR analysis of MAG.<sup>2,16</sup> These relative rates were converted to absolute values by multiplication with GP:

$$\text{Total gluconeogenesis} = H5/H2 \times \text{GP}$$

$$\text{Gluconeogenesis from glycerol} = [(H5-H6S)/H2] \times \text{GP}$$

$$\text{Gluconeogenesis from Krebs cycle} = H6S/H2 \times \text{GP}$$

$$\text{Glycogenolysis} = (1 - H5/H2) \times \text{GP}.$$

## RESULTS AND DISCUSSION

### Analysis of glucose isotopomers by $^{13}\text{C}$ NMR of MAG

$^{13}\text{C}$  NMR spectroscopy of MAG in acetonitrile yields significant advantages for analysis of glucose  $^{13}\text{C}$ -isotopomers compared with conventional  $^{13}\text{C}$  NMR spectroscopy of glucose in aqueous solution. As MAG, each hexose carbon is represented by a single well-resolved resonance and narrow  $^{13}\text{C}$  linewidths of 0.5–0.8 Hz are routinely obtained. The low salt content allows effective and reproducible implementation of observe and decoupling pulses. MAG carbons exhibit  $^{13}\text{C}$ – $^{13}\text{C}$  coupling with nearest neighbors and also with more distant carbons (see Table 1), providing the basis for resolving a diversity of glucose  $^{13}\text{C}$ -isotopomers by  $^{13}\text{C}$  NMR. For MAG synthesized from  $[\text{U-}^{13}\text{C}]\text{glucose}$ , all  $^{13}\text{C}$ – $^{13}\text{C}$  couplings of the hexose moiety contribute to the observed NMR multiplets. Carbon 1 is the optimum resonance for quantification of the  $[\text{U-}^{13}\text{C}]\text{glucose}$  isotopomer since it features a well-resolved quartet signal as a result of coupling to carbons 2 and 5 (see Table 1). For MAG prepared from plasma glucose, it is assumed that this quartet represents  $[\text{U-}^{13}\text{C}]\text{glucose}$  since dilution of the tracer by endogenous substrates is such that the probability of generating glucose molecules enriched in positions 1, 2 and 5 via recycling or from other pathways is negligible. The anticipated glucose triose isotopomers generated by recycling (see Fig. 1) generate a doublet signal which is resolved from the quartet assigned to  $[\text{U-}^{13}\text{C}]\text{glucose}$ . The contribution of singly-labeled carbon 1 from either  $[\text{U-}^{13}\text{C}]\text{glucose}$ , or its recycled products,\* is assumed to be insignificant. Finally, analysis of  $^{13}\text{C}$ – $^{13}\text{C}$  spin-coupled multiplets in resonances 2–6 of MAG (some of which are discernable in Fig. 2) can potentially further resolve and quantify the distribution of glucose triose  $^{13}\text{C}$ -isotopomers. However, under our study conditions, the signal-to-noise ratios of these multiplets were generally too low for reliable quantification.

\*Estimated to be  $\sim 10\%$  of the D12 signal<sup>19</sup> and therefore  $\sim 1\%$  of the natural abundance signal.

**Table 1.**  $^{13}\text{C}$  and  $^1\text{H}$ NMR chemical shifts and  $^{13}\text{C}$ – $^1\text{H}$  coupling constants for the hexose and acetone (A1, A2) moieties of monoacetone glucose under the conditions of the experiment (50°C, 90% acetonitrile/10%  $\text{H}_2\text{O}$  solvent). The quaternary carbon signal of the acetone group is not included and the absolute stereochemistry of each acetone methyl group is not assigned

|                | <sup>1</sup> H chemical shifts<br>(ppm) <sup>a</sup> | <sup>13</sup> C chemical shifts<br>(ppm) <sup>b</sup> | <sup>13</sup> C– <sup>1</sup> H coupling constants<br>(Hz) |                            | <sup>13</sup> C– <sup>13</sup> C coupling constants<br>(Hz) |                           |         |
|----------------|--|---|--|----------------------------|---|---------------------------|---------|
| 1              | 5.83   | 1   | 105.4  | <i>J</i> <sub>C1–H1</sub>  | 184.7   | <i>J</i> <sub>C1–C2</sub> | 33.6 Hz |
| 2              | 4.44   | 2   | 85.5   | <i>J</i> <sub>C2–H2</sub>  | 159.8   | <i>J</i> <sub>C2–C3</sub> | 43.2 Hz |
| 3              | 4.17   | 3   | 74.8   | <i>J</i> <sub>C3–H3</sub>  | 153.2   | <i>J</i> <sub>C3–C4</sub> | 38.0 Hz |
| 4              | 3.96   | 4   | 80.6   | <i>J</i> <sub>C4–H4</sub>  | 146.1   | <i>J</i> <sub>C4–C5</sub> | 46.2 Hz |
| 5              | 3.83   | 5   | 69.7   | <i>J</i> <sub>C5–H5</sub>  | 143.0   | <i>J</i> <sub>C5–C6</sub> | 40.8 Hz |
| 6- <i>proR</i> | 3.67   | 6   | 64.4   | <i>J</i> <sub>C6–H6R</sub> | 145.3   | <i>J</i> <sub>C1–C5</sub> | 3.9 Hz  |
| 6- <i>proS</i> | 3.53   | A1  | 26.5   | <i>J</i> <sub>C6–H6S</sub> | 145.2   | <i>J</i> <sub>C2–C4</sub> | 1.4 Hz  |
| A1             | 1.40   | A2  | 25.9   |                            |   | <i>J</i> <sub>C2–C5</sub> | 1.4 Hz  |
| A2             | 1.25   |   |  |                            |   | <i>J</i> <sub>C3–C5</sub> | 1.4 Hz  |
|                |  |   |  |                            |   | <i>J</i> <sub>C3–C6</sub> | 1.5 Hz  |
|                |  |   |  |                            |   | <i>J</i> <sub>C4–C6</sub> | 1.7 Hz  |

<sup>a</sup> Proton shifts relative to the acetonitrile methyl  $^1\text{H}$  signal at 1.94 ppm.

<sup>b</sup> Carbon shifts relative to the acetonitrile- $d_3$  cyano  $^{13}\text{C}$  signal at 118.7 ppm.

### Estimation of plasma $[\text{U-}^{13}\text{C}]$ glucose enrichment and GP by $^{13}\text{C}$ NMR

Figure 2 shows a  $^{13}\text{C}$  NMR spectrum derived from the MAG derivative of plasma glucose following infusion of  $[\text{U-}^{13}\text{C}]$ glucose. The very low  $^2\text{H}$ -enrichment levels of the methine and methylene hydrogens of plasma glucose ( $\sim 0.2$ – $0.5\%$ ) as a consequence of the ingested  $^2\text{H}_2\text{O}$  did not generate detectable levels of either  $^2\text{H}$ -isotope-shifted or  $^2\text{H}$ – $^{13}\text{C}$ -coupled signals in MAG.<sup>2</sup> Contributions from  $[\text{U-}^{13}\text{C}]$ glucose, represented by the Q125 quartet, were well resolved and accounted for the majority of the carbon 1 resonance. For each subject, the coefficient of

variation for the estimates of  $[\text{U-}^{13}\text{C}]$ glucose enrichment obtained from sequential blood samples averaged 5% (range 1–11%) indicating steady-state levels of  $[\text{U-}^{13}\text{C}]$ glucose. Contributions from glucose recycling, represented by the D12 doublet, accounted for only 5–10% of the carbon 1 resonance (see Table 2). The relatively low abundance of recycled  $^{13}\text{C}$  is consistent with extensive dilution at several points in the Cori cycle<sup>9</sup> and by unlabeled hepatic precursors of glucose.<sup>13</sup> Estimates of carbon 1 fractional  $^{13}\text{C}$ -enrichment and that of  $[\text{U-}^{13}\text{C}]$ glucose are listed in Table 2. In five selected samples, carbon 1 fractional  $^{13}\text{C}$ -enrichment values obtained by  $^{13}\text{C}$  NMR were identical to those obtained by  $^1\text{H}$  NMR analysis (data not shown). This agreement supports the validity of the method of Brainard *et al.*<sup>18</sup> for measuring fractional  $^{13}\text{C}$ -enrichment directly from the  $^{13}\text{C}$  NMR spectrum under the conditions of our study.

From the  $^{13}\text{C}$  NMR data, estimates of GP were obtained (Table 3), which are in good agreement with recent NMR and MS measurements.<sup>2,8,13</sup> Our estimates are also concordant with the study of Brainard *et al.*<sup>18</sup> Here, plasma glucose was analyzed directly following  $[\text{U-}^{13}\text{C}]$ glucose infusion in a single overnight-fasted healthy subject and the contribution of recycled  $^{13}\text{C}$  was not resolved from that of the infused  $[\text{U-}^{13}\text{C}]$ glucose. The agreement between our data and that of Brainard *et al.* is not surprising given the relatively low levels of recycled  $^{13}\text{C}$  isotopomers compared with those of  $[\text{U-}^{13}\text{C}]$ glucose. If the contribution of recycled  $^{13}\text{C}$  is added to that of  $[\text{U-}^{13}\text{C}]$ glucose, it results in a 9–15% inflation of  $[\text{U-}^{13}\text{C}]$ glucose enrichment, and a corresponding 9–15% underestimation of GP. However, this error will be compounded if glucose recycling is high, or if there is less dilution of  $^{13}\text{C}$  from endogenous unlabeled substrates. Glucose recycling, as measured with  $[\text{U-}^{13}\text{C}]$ glucose, has been shown to be significantly increased in patients with cancer and type-2 diabetes.<sup>20–22</sup>

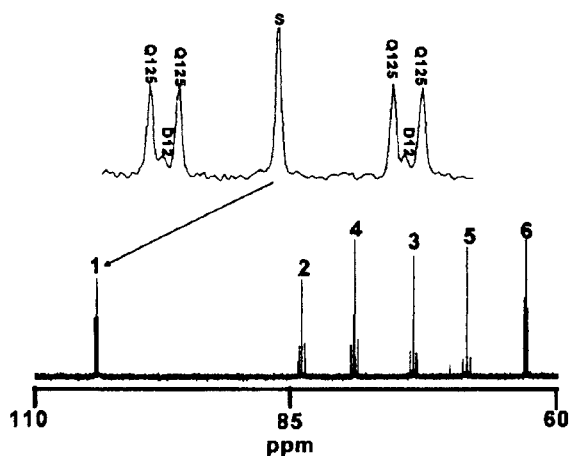


**Figure 2.**  $^{13}\text{C}$  NMR spectrum of MAG. The number above each signal refers to its position in the original glucose molecule. The multiplet of carbon 1 is shown in the expanded inset. S = natural abundance singlet; D12 = doublet from coupling between carbons 1 and 2; Q125 = quartet from coupling between carbons 1, 2 and 5. The spectrum represents the sum of 25000 free-induction decays (17.8 h)

**Table 2.**  $^{13}\text{C}$  isotopomer analysis of the C1 signal of MAG prepared from plasma glucose and the estimated contributions of [U- $^{13}\text{C}$ ]glucose,  $^{13}\text{C}$  recycled via the Cori cycle, and natural abundance  $^{13}\text{C}$  to plasma glucose enrichment

| Subject | Fractional contribution of multiplet components to <sup>13</sup> Cl signal |               |               | Contribution of infused [U- <sup>13</sup> C]glucose and recycled <sup>13</sup> C tracer to C1 glucose enrichment (%) |                             |  |  |
|---------|--|---------------|---------------|--|-----------------------------|--|--|
|         | S  | Q125          | D12           | Natural abundance  | [U- <sup>13</sup> C]glucose | Recycled <sup>13</sup> C: [1,2- <sup>13</sup> C <sub>2</sub> ] + [1,2,3,- <sup>13</sup> C <sub>3</sub> ] glucose | Total <sup>13</sup> C enrichment of carbon 1 |
| 1       | 0.270 ± 0.002  | 0.670 ± 0.004 | 0.059 ± 0.007 | 1.11   | 2.75 ± 0.01                 | 0.25 ± 0.06  | 4.11 ± 0.04                                  |
| 2       | 0.209 ± 0.022  | 0.702 ± 0.004 | 0.089 ± 0.018 | 1.11   | 3.73 ± 0.41                 | 0.49 ± 0.14  | 5.33 ± 0.56                                  |
| 3       | 0.248 ± 0.015  | 0.657 ± 0.019 | 0.094 ± 0.016 | 1.11   | 2.94 ± 0.22                 | 0.43 ± 0.09  | 4.48 ± 0.26                                  |
| 4       | 0.259 ± 0.003  | 0.685 ± 0.020 | 0.056 ± 0.017 | 1.11   | 2.94 ± 0.12                 | 0.24 ± 0.07  | 4.29 ± 0.05                                  |
| 5       | 0.245 ± 0.007  | 0.694 ± 0.001 | 0.061 ± 0.006 | 1.11   | 3.14 ± 0.09                 | 0.28 ± 0.04  | 4.54 ± 0.13                                  |

**Table 3.**  $^2\text{H}$  enrichment ratios of hydrogen 2,5 and 6S of plasma glucose (H2, H5 and H6S, respectively) derived from the relative areas of the  $^2\text{H}$  NMR signals of MAG. The fractional contribution of glycogen, glycerol and Krebs cycle to GP estimated from the  $^2\text{H}$ -enrichment ratios is also shown. Enrichment of glucose hydrogen 2 is arbitrarily set to 1.0

| Subject        | $^2\text{H}$ enrichment ratios of plasma glucose |      |      | Fractional contribution of substrates to GP (%) |          |             |
|----------------|--|------|------|---|----------|-------------|
|                | H2   | H5   | H6S  | Glycogen  | Glycerol | Krebs cycle |
| 1 <sup>a</sup> | 1.00   | 0.57 | 0.56 | 43  | 1        | 56          |
| 2              | 1.00   | 0.59 | 0.58 | 41  | 1        | 58          |
| 3 <sup>a</sup> | 1.00   | 0.55 | 0.45 | 45  | 10       | 45          |
| 4              | 1.00   | 0.51 | 0.40 | 49  | 11       | 40          |
| 5              | 1.00   | 0.50 | 0.36 | 50  | 14       | 36          |

<sup>a</sup> Values derived from a single NMR spectrum of two to three pooled MAG samples.

**Table 4.** Estimates of GP from glycogen, glycerol and the Krebs cycle from the integration of  $^2\text{H}$ - and  $[\text{U}-^{13}\text{C}]$ glucose enrichment measurements of plasma glucose

| Subject   | $[\text{U}-^{13}\text{C}]$ Glucose infusion rate (mg/kg/min) | GP (mg/kg/min) | GP from Glycogen (mg/kg/min) | Total GNG (mg/kg/min) | GP from Glycerol (mg/kg/min) | GP from Krebs cycle (mg/kg/min) |
|-----------|--|----------------|------------------------------|-----------------------|------------------------------|---------------------------------|
| 1         | 0.046  | 1.60 ± 0.01    | 0.69                         | 0.91                  | 0.02                         | 0.89                            |
| 2         | 0.071  | 1.80 ± 0.21    | 0.74                         | 1.06                  | 0.02                         | 1.04                            |
| 3         | 0.066  | 2.15 ± 0.18    | 0.97                         | 1.18                  | 0.22                         | 0.96                            |
| 4         | 0.060  | 1.93 ± 0.07    | 0.95                         | 0.98                  | 0.21                         | 0.77                            |
| 5         | 0.065  | 2.00 ± 0.07    | 1.00                         | 1.00                  | 0.26                         | 0.74                            |
| Mean ± SD | 0.062 ± 0.010  | 1.90 ± 0.19    | 0.87 ± 0.14                  | 1.03 ± 0.10           | 0.15 ± 0.12                  | 0.88 ± 0.13                     |

### $^2\text{H}$ enrichment information from $^2\text{H}_2\text{O}$ and integration with estimates of GP from $[\text{U}-^{13}\text{C}]$ glucose

The  $^2\text{H}_2\text{O}$  enrichment data and fractional gluconeogenic rates from these subjects as measured by  $^2\text{H}$  NMR analysis of MAG have been reported in a separate account.<sup>23</sup> A representative  $^2\text{H}$  NMR spectrum of MAG demonstrating the typical distribution of  $^2\text{H}$  signal intensities in the glucose hexose skeleton is shown in Fig. 3. The relative enrichment of hydrogens 2, 5 and 6S of glucose are obtained by quantifying the relative areas of the respective signals in the spectrum.<sup>2,16,23</sup> For two of the subjects, derivatization of glucose to MAG was incomplete; hence blood samples were pooled to obtain spectra with acceptable signal-to-noise. For the three remaining subjects, a set of three deuterium spectra were obtained. For each of these subjects, the coefficient of variance associated with the hydrogen 5/hydrogen 2 and hydrogen 6S/hydrogen 2 enrichment ratio measurement was ~10%. For the group of five subjects, the enrichment of glucose hydrogen 2 was estimated to be  $98 \pm 7\%$  that of body water, indicating that all plasma glucose molecules had undergone complete exchange of hydrogen 2 and body water via interconversion of glucose-6-phosphate and fructose-6-phosphate.<sup>1</sup> The relative  $^2\text{H}$ -enrichments of positions 2, 5 and 6S and the

fractional contribution of glycogen and gluconeogenic substrates to GP calculated from this data are summarized in Table 4. The data show that at 16 h of fasting, gluconeogenesis accounts for ~50% of GP, with anaplerotic outflow from the Krebs cycle contributing the bulk of gluconeogenic flux with only minor contributions from glycerol. These values are in good agreement with recent NMR and MS measurements.<sup>1,2</sup> The relative rates of gluconeogenesis and glycogenolysis were converted to absolute flux values by multiplication with GP and these absolute flux values are presented in Table 3.

Under the conditions of this study, estimates of glycerol gluconeogenesis are associated with relatively high

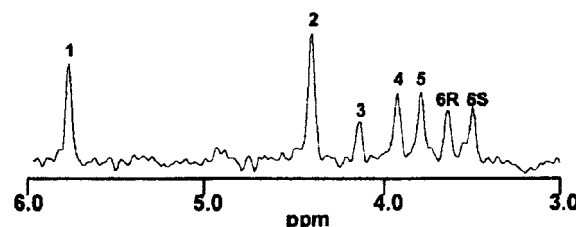


**Figure 3.**  $^2\text{H}$  NMR spectrum of MAG prepared from a single plasma glucose blood sample of subject 4. The number above each signal represents its position in the glucose skeleton. The spectrum represents 53 850 free-induction decays for a total collection time of ~18 h

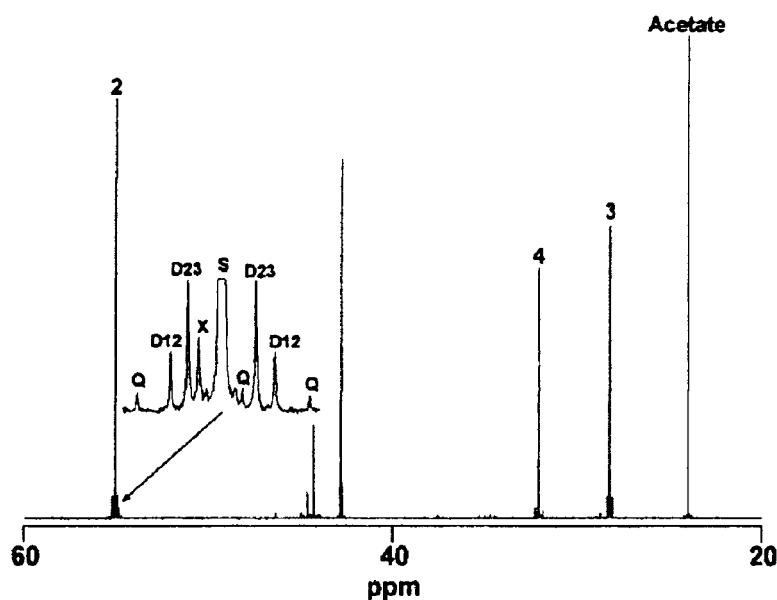


**Figure 4.**  $^{13}\text{C}$  NMR spectrum of phenylacetylglutamine from subject 2 featuring the resonances of carbons 2, 3 and 4 of the glutamine moiety (labeled 2, 3 and 4). The multiplet of carbon 2 is shown in expanded form and the components labeled as follows: S = singlet component; D12 = doublet from coupling between carbons 1 and 2; D23 = doublet from coupling between carbons 2 and 3; Q = quartet from coupling between carbons 1, 2 and 3; X = unknown signal that coincides with one of the quartets. The spectrum represents the sum of 25000 free-induction decays (17.8 h)

levels of uncertainty (note the range and standard deviation for glycerol gluconeogenesis in Table 3 and 4). This is partly due to the fact that the fractional contribution of glycerol to GP is obtained by subtraction of two signals of comparable intensities (hydrogen 5 and 6S) that are associated with noise levels of  $\sim 10\%$ . In addition, some of the difference in  $^2\text{H}$  enrichment between hydrogens 5 and 6S of glucose may be due to incomplete exchange of hydrogen between water and gluconeogenic precursors that pass through the Krebs cycle.<sup>2</sup> This results in an overestimate of glycerol gluconeogenesis and a corresponding underestimate of gluconeogenesis from the Krebs cycle. Note that this latter uncertainty cannot be minimized by improving the signal to noise ratio of the  $^2\text{H}$  NMR spectrum.

### PAGN enrichment and $^{13}\text{C}$ -isotomer distributions from $[\text{U-}^{13}\text{C}]\text{glucose}$

Generally, excess  $^{13}\text{C}$ -enrichment levels in the glutamine carbons of PAGN following  $[\text{U-}^{13}\text{C}]\text{glucose}$  administration were very low, ranging from 0.1 to 0.2% for carbons 2 and 3 and  $\sim 0.05\%$  for carbon 4. These enrichment levels were lower than that of the recycled glucose isotopomers indicating incomplete equivalence of  $^{13}\text{C}$ -enrichment between oxaloacetate (OAA) of the hepatic Krebs cycle and the OAA moiety of glutamine. This is probably due to dilution of  $^{13}\text{C}$ -glutamine derived from

the hepatic Krebs cycle by the influx of unlabeled glutamine from peripheral tissues.<sup>24–27</sup> Not surprisingly, the largest multiplet contributions was derived from subject 2, who received the highest infusion rate of  $[\text{U-}^{13}\text{C}]\text{glucose}$  (0.071 mg/kg/min), and is shown in Fig. 4. PAGN spectra from the remaining subjects had somewhat lower multiplet intensities. Generally, while individual multiplet components had adequate signal-to-noise ratios (see inset of Fig. 4), they were difficult to quantify due their small size in comparison to the large central singlet signal. In particular, they were highly susceptible to minor shimming maladjustments, including artifact signals from spinning sidebands. Furthermore, as a consequence of the very low levels of excess  $^{13}\text{C}$ -enrichment from the tracer, the multiplets contain significant contributions from natural abundance  $^{13}\text{C}$ – $^{13}\text{C}$  isotopomers, present at  $\sim 0.011\%$ . For the carbon 2 resonance, these were estimated to account for 10% of the D23, and 25% of the D12 signal while for the carbon 4 resonance, they accounted for 14% of the doublet signal.\* Uncorrected, these natural abundance contributions would substantially distort metabolic flux estimates derived from the multiplet intensities. Nevertheless, Fig. 4 demonstrates the potential of obtaining PAGN  $^{13}\text{C}$ -isotomer information from a primed infusion of

\*The contribution was estimated by multiplying the relative area of the central singlet by 0.011 and comparing this value with the relative areas of the multiplets.



[U-<sup>13</sup>C]glucose and qualitatively reveals some important characteristics of hepatic Krebs cycle fluxes. In the carbon 2 multiplet, the intensity of the D23 signal clearly exceeds that of the quartet (Q), indicating a substantial excess of [2,3-<sup>13</sup>C<sub>2</sub>]glutamine over [1,2,3-<sup>13</sup>C<sub>3</sub>]glutamine. This is consistent with extensive cycling of carbons between pyruvate and OAA<sup>19</sup> and is in agreement with the glutamine <sup>13</sup>C-isotopomer distribution following metabolism of [U-<sup>13</sup>C]propionate.<sup>19</sup> The presence of a doublet corresponding to [4,5-<sup>13</sup>C<sub>2</sub>]glutamine in the carbon 4 signal indicates entry of [U-<sup>13</sup>C]acetyl-CoA into the cycle, presumably from oxidation of [U-<sup>13</sup>C]pyruvate via pyruvate dehydrogenase.

The multiplet information from carbons 2, 3 and 4 of PAGN therefore provide the basis for describing hepatic anaplerotic, oxidative and pyruvate recycling fluxes. This analysis assumes that the <sup>13</sup>C-isotopomer distribution of PAGN is entirely derived from the hepatic Krebs cycle. Since the liver also receives glutamine from peripheral tissues, notably skeletal muscle, the possibility exists that <sup>13</sup>C-enriched glutamine could be produced via peripheral oxidation of [U-<sup>13</sup>C]glucose, then exported to the liver and incorporated into PAGN. This would distort the observed <sup>13</sup>C-isotopomer distribution because anaplerotic and pyruvate recycling activities are much smaller in muscle compared to liver. In principle, the extent of such extra-hepatic contributions can be gauged by comparing the PAGN isotopomer distribution derived from [U-<sup>13</sup>C]glucose with that obtained from a more specific hepatic tracer, such as [U-<sup>13</sup>C]lactate or [U-<sup>13</sup>C]alanine.

Assuming that PAGN excess <sup>13</sup>C-enrichment and <sup>13</sup>C NMR multiplet intensities increase linearly with the rate of [U-<sup>13</sup>C]glucose infusion, we anticipate that a doubling of the glucose infusion rates used in this study to ~0.12–0.15 mg/kg/min (~3 g of [U-<sup>13</sup>C]glucose per subject) would be sufficient to routinely provide good-quality PAGN isotopomer information by <sup>13</sup>C NMR. Meanwhile, these higher infusion rates would generate plasma [U-<sup>13</sup>C]glucose enrichment levels of 5–6%; sufficiently dilute for estimating GP with the current approach. Additionally, the application of new indirect detection methods such as the J-resolved HSQC procedure<sup>28</sup> would eliminate spinning sideband artifacts while substantially improving the sensitivity of the <sup>13</sup>C-isotopomer measurements.

In summary, we developed a highly practical method for quantifying GP and absolute gluconeogenic and glycogenolytic fluxes by NMR analysis of a single convenient derivative of plasma glucose following administration of [U-<sup>13</sup>C]glucose and <sup>2</sup>H<sub>2</sub>O. We also demonstrated the potential for obtaining complementary hepatic Krebs cycle fluxes by noninvasive analysis of hepatic glutamine isotopomers from a single additional urine sample. The approach could be valuable for obtaining a detailed assessment of hepatic glucose and Krebs cycle metabolism in a standard hospital setting.

## Acknowledgements

We are pleased to acknowledge the excellent technical assistance and support provided by Jose Alves and the nursing staff of the University Hospital of Coimbra. This work was supported through a European Community Marie Curie Experienced Researcher Fellowship (MCFI-2000-00148) (JGJ) and the Portuguese Foundation of Science and Technology.

## REFERENCES

- Chandramouli V, Ekberg K, Schumann WC, Kalhan SC, Wahren J, Landau BR. Quantifying gluconeogenesis during fasting. *Am. J. Physiol.* 1997; **273**: E1209–E1215.
- Jones JG, Solomon MA, Cole SM, Sherry AD, Malloy CR. An integrated <sup>2</sup>H and <sup>13</sup>C NMR study of gluconeogenesis and TCA cycle flux in humans. *Am. J. Physiol.* 2001; **281**: E848–E851.
- Landau BR, Wahren J, Chandramouli V, Schumann WC, Ekberg K, Kalhan SC. Contributions of gluconeogenesis to glucose production in the fasted state. *J. Clin. Invest.* 1996; **98**: 378–385.
- Saadatian M, Peroni O, Diraison F, Beylot M. In vivo measurement of gluconeogenesis in animals and humans with deuterated water: a simplified method. *Diabetes. Metab.* 2000; **26**: 202–209.
- Schumann WC, Gastaldelli A, Chandramouli V, Previs SF, Pettiti M, Ferrannini E, Landau BR. Determination of the enrichment of the hydrogen bound to carbon 5 of glucose on (H<sub>2</sub>O)-H-2 administration. *Anal. Biochem.* 2001; **297**: 195–197.
- Schleucher J, Vanderveer P, Markley JL, Sharkey TD. Intramolecular deuterium distributions reveal disequilibrium of chloroplast phosphoglucose isomerase. *Plant Cell Environ.* 1999; **22**: 525–533.
- Schleucher J, Vanderveer P, Sharkey TD. Export of carbon from chloroplasts at night. *Plant Physiol.* 1998; **18**: 1439–1445.
- Katz J, Tayek JA. Gluconeogenesis and the Cori cycle in 12-, 20-, and 40-h-fasted humans. *Am. J. Physiol.* 1998; **275**: E537–E542.
- Mao CS, Bassilian S, Lim SK, Lee WNP. Underestimation of gluconeogenesis by the [U-<sup>13</sup>C<sub>6</sub>]glucose method: effect of lack of isotope equilibrium. *Am. J. Physiol.* 2002; **282**: E376–E385.
- Katz J, Tayek JA. Recycling of glucose and determination of the Cori Cycle and gluconeogenesis. *Am. J. Physiol.* 1999; **277**: E401–E407.
- Kelleher JK. Estimating gluconeogenesis with [U-<sup>13</sup>C]glucose: molecular condensation requires a molecular approach. *Am. J. Physiol.* 1999; **277**: E395–E400.
- Radziuk J, Lee WNP. Measurement of gluconeogenesis and mass isotopomer analysis based on [U-<sup>13</sup>C]glucose. *Am. J. Physiol.* 1999; **277**: E199–E207.
- Landau BR, Wahren J, Ekberg K, Previs SF, Yang DW, Brunengraber H. Limitations in estimating gluconeogenesis and Cori cycling from mass isotopomer distributions using [U-<sup>13</sup>C<sub>6</sub>]glucose. *Am. J. Physiol.* 1998; **274**: E954–E961.
- Wykes LJ, Jahoor F, Reeds PJ. Gluconeogenesis measured with [U-<sup>13</sup>C]glucose and mass isotopomer analysis of apoB-100 amino acids in pigs. *Am. J. Physiol.* 1998; **274**: E365–E376.
- Dugelay S, Yang D, Soloviev MV, Previs SF, Agarwal KC, Fernandez CA, Brunengraber H. Assay of the concentration and <sup>13</sup>C-labeling pattern of phenylacetylglutamine by nuclear magnetic resonance. *Anal. Biochem.* 1994; **221**: 368–373.
- Jones JG, Perdigoto R, Rodrigues TB, Geraldes CFGC. Quantitation of absolute <sup>2</sup>H enrichment of plasma glucose by <sup>2</sup>H NMR analysis of its monoacetone derivative. *Magn. Reson. Med.* 2002; **48**: 535–539.
- Jones JG, Carvalho RA, Franco B, Sherry AD, Malloy CR. Measurement of hepatic glucose output, Krebs cycle, and gluconeogenic fluxes by NMR analysis of a single plasma glucose sample. *Anal. Biochem.* 1998; **263**: 39–45.
- Brainard JR, Downey RS, Bier DM, London RE. Use of multiple <sup>13</sup>C-labeling strategies and <sup>13</sup>C NMR to detect low levels of exogenous metabolites in the presence of large endogenous pools:

- measurement of glucose turnover in a human subject. *Anal. Biochem.* 1989; **176**: 307–312.
19. Jones JG, Naidoo R, Sherry AD, Jeffrey FMH, Cottam GL, Malloy CR. Measurement of gluconeogenesis and pyruvate recycling in the rat liver: a simple analysis of glucose and glutamate isotopomers during metabolism of [1,2,3-<sup>13</sup>C<sub>3</sub>]propionate. *FEBS Lett.* 1997; **412**: 131–137.
  20. Tayek JA, Katz J. Glucose production, recycling, and gluconeogenesis in normals and diabetics: a mass isotopomer [U-<sup>13</sup>C]glucose study. *Am. J. Physiol.* 1996; **270**: E709–E717.
  21. Tayek JA, Katz J. Glucose production, recycling, Cori cycle, and gluconeogenesis in humans: relationship to serum cortisol. *Am. J. Physiol.* 1997; **272**: E476–E484.
  22. Richardson AP, Tayek JA. Type 2 diabetic patients may have a mild form of an injury response: a clinical research center study. *Am. J. Physiol.* 2002; **282**: E1286–E1290.
  23. Jones JG, Rodrigues TB, Geraldine CFGC, Perdigoto RA. (Abstract). *Proc. Int. Soc. Magn. Reson. Med.* 2002; **10**: 2194, 2002.
  24. Matthews DE, Marano MA, Campbell RG. Splanchnic bed utilization of glutamine and glutamic acid in humans. *Am. J. Physiol.* 1993; **264**: E848–E854.
  25. Nurjhan N, Bucci A, Perriello G, Stumvoll M, Dailey G, Bier DM, Toft I, Jenssen TG, Gerich JE. Glutamine—a major gluconeogenic precursor and vehicle for interorgan carbon transport in Man. *J. Clin. Invest.* 1995; **95**: 272–277.
  26. Diraison F, Large V, Brunengraber H, Beylot M. Non-invasive tracing of liver intermediary metabolism in normal subjects and in moderately hyperglycaemic NIDDM subjects. Evidence against increased gluconeogenesis and hepatic fatty acid oxidation in NIDDM. *Diabetologia* 1998; **41**: 212–220.
  27. Diraison F, Large V, Maugeais C, Krempf M, Beylot M. Non-invasive tracing of human liver metabolism: comparison of phenylacetate and apoB-100 to sample glutamine. *Am. J. Physiol.* 1999; **277**: E529–E536.
  28. Burgess SC, Carvalho RA, Merritt ME, Jones JG, Malloy CR, Sherry AD. <sup>13</sup>C isotopomer analysis of glutamate by J-resolved heteronuclear single quantum coherence spectroscopy. *Anal. Biochem.* 2001; **289**: 187–195.
  29. Katz J, Wals P, Lee WNP. Isotopomer studies of gluconeogenesis and the Krebs cycle with <sup>13</sup>C-labeled lactate. *J. Biol. Chem.* 1993; **268**: 25509–25521.
  30. Des Rosiers C, Di Donato L, Comte B, Laplante A, Marcoux C, David F, Fernandez CA, Brunengraber H. Isotopomer analysis of citric acid cycle and gluconeogenesis in rat liver. Reversibility of isocitrate dehydrogenase and involvement of ATP-citrate lyase in gluconeogenesis. *J. Biol. Chem.* 1995; **270**: 10027–10036.